Research Square

Preprints are preliminary reports that have not undergone peer review.
They should not be considered conclusive, used to inform clinical practice,
or referenced by the media as validated information.

Deglaciation creates contested socio-ecological frontiers in the European Alps

Arthur BAYLE

arthur.bayle.env@gmail.com

Univ. Grenoble Alpes, Univ. Savoie Mont Blanc, CNRS, LECA https://orcid.org/0000-0002-3442-0789

Adrien Guerou

USMB/INRAE

Mauro Fischer

University of Bern https://orcid.org/0000-0002-0950-776X

Florent Arthaud

Université Savoie Mont Blanc, INRAE, CARRTEL

Sophie Cauvy-Fraunié

INRAE https://orcid.org/0000-0001-8600-0519

Jean-Christophe Clément

Université Savoie Mont Blanc https://orcid.org/0000-0002-0841-7199

Jacques Mourey

ASTER-CEN 74

Jérôme Poulenard

EDYTEM, Université Savoie Mont-Blanc, CNRS https://orcid.org/0000-0003-0810-0308

Philippe Billet

Universite Jean Moulin Lyon III

Matthias Huss

3 Laboratory of Hydraulics, Hydrology and Glaciology (VAW), ETH Zürich

Jean-Baptiste Bosson

Conservatory of natural areas of Haute-Savoie (Asters) https://orcid.org/0000-0003-4732-4945

Article

Keywords:

Posted Date: August 28th, 2026

DOI: https://doi.org/10.21203/rs.3.rs-8871146/v1

License: This work is licensed under a Creative Commons Attribution 4.0 International License.
Read Full License

Additional Declarations: There is **NO** Competing Interest.

Deglaciation creates contested socio-ecological frontiers in the European Alps

Adrien Guérou[1*✉], Arthur Bayle[2,3*✉], Mauro Fischer[4,5], Florent Arthaud[1,6], Sophie Cauvy-Fraunié[7], Jean-Christophe Clément[1], Jacques Mourey[8], Jérôme Poulenard[9], Philippe Billet[10,11], Matthias Huss[12,13,14], Jean-Baptiste Bosson[15]

[1] Univ. Savoie Mont Blanc, INRAE, CARRTEL, 74200, Thonon-Les-Bains, France
[2] Climate Change Impacts and Risks in the Anthropocene (C-CIA), Institute for Environmental Sciences, University of Geneva, 66 Bvd Carl-Vogt, CH-1205 Geneva, Switzerland
[3] Department F.-A. Forel for Environmental and Aquatic Sciences, University of Geneva, 66 Boulevard Carl Vogt, CH-1205 Geneva, Switzerland
[4] Institute of Geography, University of Bern, Bern, Switzerland
[5] Oeschger Centre for Climate Change Research, University of Bern, Bern, Switzerland
[6] Service EcoAqua, Direction de la Recherche et de l'Appui Scientifique, OFB, Thonon-Les-Bains, France
[7] INRAE, UR RIVERLY, Centre de Lyon-Villeurbanne, Villeurbanne, France
[8] Asters-CEN 74
[9] EDYTEM, Univ. Savoie Mont Blanc, CNRS, 73000, Chambéry, France
[10] Institut de droit de l'environnement, Faculté de Droit, Université Jean Moulin Lyon III
[11] CNRS - UMR 5600 - EVS-IDE
[12] Laboratory of Hydraulics, Hydrology and Glaciology (VAW), ETH Zürich, Zürich, Switzerland
[13] Swiss Federal Institute for Forest, Snow and Landscape Research (WSL), Sion, Switzerland
[14] Department of Geosciences, University of Fribourg, Fribourg, Switzerland
[15] Marge Sauvage, Annecy, France

* First authors

✉ Corresponding authors

Rapid glacier retreat is transforming mountain landscapes, exposing terrain where postglacial ecosystems emerge while new opportunities for infrastructure development also arise. These newly ice-free areas are therefore becoming socio-ecological frontiers in which ecosystem development, land use and conservation frameworks increasingly overlap. Yet spatially explicit evidence of where these overlaps occur remains scarce, limiting the ability of governance systems to anticipate emerging conflicts. Here, using the European Alps as a data-rich case study, we pair satellite-derived land cover mapping with inventories of ski infrastructure, hydropower reservoirs and protected areas within the end-of-Little Ice Age glacier footprint. We show that newly exposed terrain already contains emerging vegetated and freshwater habitats, whose regional distribution is mainly modulated by temperature gradients. Concomitantly, ski and hydropower infrastructures already occupy parts of postglacial terrain, even within strictly protected areas, revealing mismatches between formal conservation status and land-use decisions. Emerging postglacial ecosystems fall into a de facto legal vacuum, as current tools encourage reactive, piecemeal decisions that fail to safeguard ecosystem functions and services. We argue for anticipatory stewardship that recognizes glacier and postglacial ecosystems in law and planning as a single transforming system. These regional findings foreshadow a global governance challenge that will intensify as deglaciation expands in regions where deglaciation exposes land to competing ecological, economic and political interests.

Human prosperity is inherently tied to the use of natural resources, yet this dependence increasingly conflicts with the need to safeguard the ecosystems that sustain it[1]. Nature conservation has largely focused on protecting established and well-characterized ecosystems, leaving those still forming—or yet to appear—outside existing frameworks. As anthropogenic climate change rapidly reshapes Earth's surface[2], new ecosystems are appearing in exposed environments[3], challenging conservation frameworks designed for stable baselines. Following centuries of conditions favorable to glaciers during the Little Ice Age (LIA)[4], warming since the industrial era (1850-1900) has triggered their widespread retreat worldwide[5]. Among its cascading consequences, deglaciation has exposed terrain unseen for centuries to millennia, where pristine terrestrial[6], freshwater and marine ecosystems[7] are now forming, which in turn influence Earth's functioning and human societies[8].

While glacier shrinkage has major and worrying ecological and social consequences from local to global scale[9], postglacial ecosystems have ecological values and provide ecosystem services—including biodiversity refugia[10], geodiversity[11], freshwater retention[12] and carbon storage[3] —and have recently been formally recognized as conservation priorities at the international level[13]. Yet, once they emerge, many of these former glacier beds are threatened by infrastructure development such as mining[14], hydropower [15], or ski resorts[16], thereby jeopardizing the long-term evolution of deglaciated areas. As a result, postglacial terrains—often regarded as empty or transitional spaces—are emerging as a new frontier where ecosystem development and economic interests increasingly collide, fueling societal tension (**Fig. 1**).

Ecological succession following glacier retreat has been extensively studied at local to global scales[17], and glacier retreat has also long been recognized as a social process that reshapes perceptions, values, cultural meanings, economic interests and relations among actors operating at different scales[18]. Recent work has further emphasized the need for stewardship of deglaciated lands[19-21], while regional studies have assessed the socio-environmental value, risks and management potential of specific postglacial components such as glacier lakes. Yet the spatial intersection between postglacial habitat emergence, infrastructure occupation and conservation coverage remains poorly quantified across entire mountain ranges. This limits our ability to identify where deglaciation is already producing contested socio-ecological frontiers, and where governance systems may need to respond before land-use decisions become irreversible. Recent advances in remote sensing and glaciological modeling have improved our understanding of glacier evolution and its ecological cascades[22], but we still lack a clear picture of where postglacial ecosystems are developing and which habitats they comprise. This gap persists because end-of-LIA glacier extents are still incomplete[23] and postglacial habitats have, until recently, been difficult to resolve with satellite remote sensing. Likewise, records of socio-economic activities expanding over deglaciated areas are missing or fragmented across administrative or commercial datasets.

Here, we address this gap in the European Alps by jointly mapping the present-day postglacial land cover, major high-mountain infrastructures and conservation coverage within the end-of-LIA glacier extent. The European Alps—still hosting over 3,000 retreating glaciers[24] and marked by dense human activity[25]—provide a data-rich regional case study in which glacier retreat, ski tourism, hydropower development and multiple conservation instruments coexist within a relatively well-documented mountain range, as the region is experiencing the fastest relative glacier loss[5]. We combine recently reconstructed LIA glacier outlines with satellite-derived land cover and inventories of ski and hydropower infrastructures. By comparing these intersections with the main conservation and legal instruments in force at international, European Union and national levels, we quantify where ecosystem emergence, infrastructure occupation

and protection gaps currently coincide, and use this diagnosis to discuss principles for anticipatory stewardship of rapidly evolving glacier-to-postglacial systems.

Present-day postglacial ecosystems mapping and patterns

We mapped the present-day land cover within the end-of-LIA glacier extent[23] across the European Alps using pigment-sensitive phenological indices derived from all clear-sky summer Sentinel-2 images (20 m resolution) acquired between 2017 and 2023 (see Methods). Six ecologically relevant land-cover classes were mapped using a random-forest classifier trained and cross-validated with a fourfold spatial-split design and then related to topographic and climatic variables to describe regional patterns of postglacial land cover (see Methods). Classification uncertainty was quantified with conformal statistics, providing pixel-level confidence scores and aggregated uncertainty ranges for each class. The analysis was restricted to terrain that deglaciated up to 2015, corresponding to the latest consistent alpine wide glacier inventory[26].

At the end of the LIA, around 1850, glaciers of the European Alps covered 4,289 km² (**Fig. 2**, Table S1). By 2015, ice extent had declined to 1,783 km² (–58%), exposing 2,506 km² of new area. Of this deglaciated area, 93% (2,336 ± 1 km²) is mapped as bare land, 6% (155 ± 7 km²) as terrestrial vegetation, and 0.6% (15 km²) as freshwater bodies. These proportions are conservative: the bare land class likely contains very sparse pioneer vegetation below the 20 m sensor resolution (<10% vegetation cover[27]). A 50 cm NDVI-derived vegetation cover analysis over the Mont-Blanc massif confirmed this interpretation: 12.8% of bare-land pixels contained detectable vegetation cover, generally in very low proportions, while sparse vegetation and grassland contained on average 17.3% [9–28%] and 45% [23–67%] vegetation cover, respectively (Fig. S9). Our water mapping also underestimates the detection of very small water bodies (<0.01 km²; see Methods, Fig. S11). Within the mapped vegetated terrain, grasslands (100 ± 4 km²) and sparse vegetation (44 km²) account for 92 ± 2%, whereas dense forests cover 11 ± 3 km² (7 ± 2%) and shrublands remain nearly absent (<1 km²). Switzerland contains the largest deglaciated surface area, while Austria exhibits the highest proportion of vegetation cover (8%), followed by Switzerland (7%), Italy (5%) and France (4%). France currently hosts the highest share of dense forests (16 ± 2% of its vegetated area), whereas proglacial areas within LIA limits in Austria are dominated by grasslands (70 ± 1%) and has minimal forest cover (<2%). These national contrasts reflect regional gradients in elevation and climate, as well as geomorphological and lithological context, which together shape the pace and structure of vegetation and lake development in postglacial ecosystem[28,29]. Natural lakes represent less than 1% of the former glaciated surface, with Switzerland hosting the largest total (~3.7 km²; Table S10). Artificial reservoirs—primarily built for hydropower—add another 3 km² in Switzerland, 1.1 km² in Italy, and 0.6 km² in Austria, jointly accounting for roughly 30% of the freshwater area within deglaciated terrain. No terrestrial vegetation or water surface has been detected in the small postglacial areas of Germany, neither of Slovenia where glaciers have completely vanished according to our reference dataset[26].

While lakes span a broad elevation range between ~1500 and 3000 m a.s.l., the altitudinal distribution of land-cover types within end-of-LIA glacier extent reveals a clear vertical zonation consistent with established alpine vegetation belts (**Fig. 3a**). Forests are widespread below 2000 m a.s.l., shrublands occupy the upslope belt, and grasslands dominate up to ~2250 m a.s.l., above which vegetation becomes increasingly sparse, and bare land prevails. Mean annual air temperature (MAAT) strongly drives this distribution (**Fig. 3b**): vegetated surfaces have a median MAAT of –1.3 °C, around 3 °C warmer than bare lands (–4.2 °C). Forests occur in the warmest sites (+1.2 °C), followed by shrublands (~0 °C), grasslands (–1.2 °C), and sparse vegetation (–2.2 °C). Bare land is found on slightly steeper slopes (~26°) than vegetated classes (~24°), with no systematic differences among vegetation types, suggesting that finer scale

biogeomorphic processes operating at meter resolution[30] are not resolved at our mapping scale (see also Table S3).

To assess whether land cover patterns in postglacial terrain have caught up with those of surrounding landscapes, we compared its land cover to adjacent areas likely ice-free during most of the Holocene (~11.000 years ago)[4] restricted to the same elevation range and mapped with the same classification processing (see Methods). Our analysis reveals systematic vegetation lags between recently deglaciated areas and adjacent terrains across the European Alps (**Fig 3a**). The median elevation of vegetation belts within postglacial ecosystems are located on average 120-170 meters lower than in adjacent terrain, with lower proportions of each vegetation types (about three times, see also Table S3). In contrast, lakes formed at slightly higher elevations (+150 m) compared to adjacent areas, with a larger relative distribution (0.6% vs 0.1%), consistent with the formation of persistent depressions near former glacier margins through geomorphic over deepening and moraine damming. Indeed, many lakes that formed following earlier phases of deglaciation have since been progressively infilled by sediments and organic matter, explaining partly their lower abundance in adjacent long-deglaciated terrain[31]. Taken together, these systematic vertical and compositional lags indicate that postglacial ecosystems remain in an early stage of development. Although time since deglaciation primarily drives postglacial ecosystem development[32], persistent paraglacial processes—slope instability, sediment remobilization, and extremely slow pedogenesis—continuously influence early-successional stages and restrict where stable soils and closed vegetation can form[17]. These constraints mean that postglacial terrains may not converge toward the structure of surrounding long-deglaciated areas, even over centuries. Instead, they may persist as distinct biogeomorphic units within mountain landscapes[33]. Although our land-cover analysis does not directly quantify species assemblages or biodiversity uniqueness, it shows that vegetated habitats in recently deglaciated terrain occur at systematically lower elevations than comparable vegetation belts in adjacent terrain. Together with existing studies on postglacial succession and geodiversity, this suggests that these areas could provide unconventional refugia for early-successional communities and associated biodiversity under continued climate warming[8]

Postglacial ecosystems value and services under pressure

Glaciers and postglacial terrains support ecological communities and ecosystem functions that are strongly shaped by cold-climate conditions, primary succession and geomorphic disturbance. Their trajectories are now diverging under climate change: glacier retreat reduces cold-dependent habitats and the services tied to ice and meltwater regimes[34], while newly exposed terrain progressively develops terrestrial and freshwater habitats, soils and biogeochemical functions[35].In parallel, postglacial ecosystems in these areas provide a variety of regulation, support, and provisional services such as freshwater retention, carbon storage, soil formation or nutrient cycling[36]. These emerging habitats do not compensate for those lost with vanishing ice, but they are becoming an increasingly important component to socio-ecological resilience in cold regions[18].

To provide first-order indicators of ecosystem-service development, we estimated two regulation services-—surface-water retention in lakes and carbon storage—based on our postglacial ecosystems land cover map. These estimates are not intended as complete ecosystem-service accounts, but as conservative, spatially explicit proxies for functions that are beginning to develop within recently deglaciated terrain. Using empirical area-volume scaling relationships, we estimate that natural postglacial lakes within the end-of-LIA glacier boundaries store $119 \pm 71 \times 10^6$ m³ of freshwater, representing only ~0.1 ± 0.1% of the ~$180 \pm 30 \times 10^9$ m³ of glacier water-content volume lost since end of LIA[23] (Fig. S12). While water storage

in emerging wetlands, soils and aquifers is not accounted for here, this low fraction indicates that most ice-meltwater is routed downstream rather than buffered in nascent lakes, and that it is lower than projected future retention of Alpine meltwater in glacial overdeepenings (0.3–0.9% for 2020–2100[3]). Carbon storage based on land-cover-derived carbon density factors (see Methods) show that postglacial ecosystems currently store ~2 ± 1 megatons of carbon (MtC), largely in bare land soils (~50%, see Table S4). While these values are modest relative to national carbon budgets[37], chrono sequence studies suggest that soil organic carbon accumulates steadily in glacier forelands, especially under warmer conditions[38]. Our estimate thus probably under-represents the full potential of these young ecosystems.

Although postglacial terrain is beginning to support ecosystem functions and services, it is also already occupied by socio-economic infrastructure, especially from the expansion of ski resorts[39] and hydropower[15]. By intersecting infrastructure datasets within the end-of-LIA glacier boundaries, we identified 52 ski resorts operating partly over these regions, comprising 605 km of groomed ski runs and 269 km of lift infrastructures (**Fig. 4**). Half of them were still located on glaciers in 2015 and half on deglaciated terrain (see also Table S8). Although these facilities represent only 2–3% of the Alpine-wide ski infrastructures, their concentration at high-elevation, geomorphically unstable terrain implies more intensive construction means and maintenance, amplifying their impacts on natural ecosystems[40]. National patterns differ: Austria retains proportionally more installations on glacierized terrain, whereas France, Switzerland and Italy have a larger share of infrastructures located on terrain that was ice-free by 2015.

We also identified 22 artificial lakes for hydropower production within areas deglaciated in the last 170 years (**Fig. 4**). Fifteen of these installations are in Switzerland, accounting alone for over 60% of the surface of artificial lakes in the newly ice-free terrain (see Table S10). Hydropower can contribute to low-carbon energy systems and water-resource management and may therefore play a role in climate-change mitigation and adaptation. However, when reservoirs are built or operated within recently deglaciated terrain, they can also inundate early successional habitats, alter pedogenesis, freshwater and terrestrial vegetation establishment, without contributing to increased aquatic biodiversity due to highly fluctuating water levels[41]. The intersection of slowly developing ecosystems and existing high-mountain infrastructure thus reveals a potential land-use trade-off. Without anticipatory governance, these trade-offs are likely to be resolved reactively, after ecological functions and land-use interests have already come into conflict.

Partial and uneven protection of glacier-to-postglacial systems

To assess how existing conservation frameworks currently cover both glaciers and postglacial landscapes they are transforming into, we intersected the end-of-LIA glacier footprint across the European Alps with international, European and national protected-area datasets[42], grouped according to their legal strength following IUCN categories (see Methods). Despite their environmental importance, our analysis shows that glaciers and postglacial ecosystems in the European Alps are only partly covered by a complex patchwork of area-based and law-based protection approaches. Solely 21% of their surface lies within strictly protected areas according to the IUCN categories (i.e. I–II, **Fig. 4**; Table S5), and 17% under moderate protection (IUCN categories III–IV). These protections evenly apply across glacier and postglacial ecosystems but vary between countries. National parks account for most of the strictly designated protection, covering respectively 100, 47, 37, 29 and 17% of the end-of-LIA glacier extent in Slovenia, France, Austria, Italy and Germany. However, 7% of the ski infrastructures within the end-of-LIA glacier outlines fall within these theoretically effective protected areas (Table S9), underscoring the gap between formal protection status and on-the-ground land-use decisions. In Switzerland, that hosts the largest share of Alpine glacier and postglacial area, less than 1% of the end-of-LIA glacier footprint has

been put within strictly protected areas (IUCN categories I-II) and only ~10% with limited legally binding character (IUCN categories III–IV), whose practical influence depends on management priorities and sectoral trade-offs.

Other area-based recognition and land-planning tools complement this patchwork of *effectively* protected areas recognized by the IUCN (categories I-IV). In the European Union, the 1992 Habitats Directive recognizes glaciers and some emerging postglacial habitats such as coniferous forests on glaciofluvial eskers, that requires their protection by EU States through the Natura 2000 network[34]. In practice, this is one-third (1434 km²) of glacial and postglacial areas in the European Alps that falls under the 1992 Habitats Directive (see Table S7). However, its effectiveness is constrained by limited resources and funding in several member States[43]. Likewise, the 1994 nature conservation protocol of the Alpine Convention acknowledges the eminent importance of glaciers and calls for their preservation, but without proposing concrete mechanisms to achieve this goal, neither considering ecosystems emerging from their retreat. At national to sub-national scales, glacial and postglacial ecosystems are mostly protected only insofar as they fall within emblematic landscapes or broad zoning schemes, rather than as ecosystems with intrinsic ecological and functional values[44]. Switzerland illustrates both the potential and limits of this imbrication of approaches: the majority (two-third) of its 2015 postglacial terrain is covered by a mosaic of national, regional and communal protection instruments with uneven formal protection levels and roughly a quarter of its LIA glacier extent benefits from international recognition, including two RAMSAR sites and two UNESCO World Heritage areas (see Tables S6-S7). Yet the land-use pressure we document in these zones (**Fig. 4**, Table S9-S10) underscores how such international and EU recognitions may provide limited leverage for preserving glaciers and postglacial ecosystems, especially when they are not matched by the climate-mitigation commitments required for their long-term preservation.

In parallel, law-based recognition of glacier and postglacial ecosystems is very limited and fragmented in national frameworks[45], partly because of the difficulty of defining them as stable legal objects[46]. Whereas glaciers are largely absent from the legal corpus in France[47], their regulation varies from state to state in Austria. In Tyrol, hosting the largest part of Austrian glaciers, the Nature Conservation Act[48] prohibits any permanent damage to glaciers, their watershed and adjacent moraines, with some exceptions for ski area security facilities. In Italy, glaciers are treated as components of downstream river systems under public water law[49], and in Switzerland, as elements of the public domain. In these cases, glaciers qualify as public assets protected through public-property laws, allowing actions for recovery and criminal penalties for damages, but without recognizing their unique ecological functions or their dynamic transformation. Postglacial ecosystems are even less explicitly addressed because they sit at the edge of what current environmental law is designed to recognize. Most legal frameworks have evolved as reactive instruments, aimed at protecting entities that are already mapped, classified, and socially or ecologically established. As a result, developing postglacial areas are only indirectly and fragmentarily covered, insofar as they progressively incorporate elements governed by existing legal regimes—such as rivers, lakes, forests, or protected species[50]. Protection thus depends on the timely identification of these components, turning species and habitat inventories into a race against time to secure legal recognition before irreversible transformation or destruction occurs[34].

More fundamentally, most conservation frameworks rely on biodiversity baselines, relatively stable habitats and established cultural or scenic values —criteria that emerging postglacial ecosystems, by definition, rarely meet at the early stages of their development. Their temporality, ecological immaturity and apparent emptiness mean they do not fit neatly into any established category: they are neither long-

recognized wilderness to preserve nor clearly developed zones to regulate. They often fall into a de facto legal vacuum, treated as *terra nullius* within land-use planning[18].

Besides existing laws weakly enforced, it reflects structural limits in frameworks that were drafted under assumptions of climatic or ecological stability, designed to safeguard already-recognized habitats and values, and poorly suited to dynamic environments such as shrinking glaciers and nascent postglacial ecosystems. Yet our mapping shows that these supposedly 'empty' zones are precisely where biodiversity, geodiversity, habitats, and associated ecosystem services are assembling—while land-use conversion accelerates through expanding infrastructures and, in some cases, contested or illegal projects[15]. In the absence of anticipatory rules, shrinking glaciers and postglacial ecosystem formation are forced to compete with human infrastructures development and typically lose.

Towards an anticipatory stewardship framework

Glaciers and their forelands are not separate objects but two phases of a single transforming system. Every tenth of a degree now determines the survival prospects of many glaciers, yet glaciers also function as powerful flagships for climate awareness, catalyzing political and societal action[44,51]. We argue that this symbolic and mobilizing power should extend explicitly to the postglacial ecosystems that succeed them: because one becomes the other, treating their protection separately—conceptually or institutionally—risks weakening both. From a legal and governance perspective, extending existing glacier-focused instruments to include their evolving forelands offers a more realistic way to acknowledge the dynamic nature of these systems than creating entirely new regimes for each stage of deglaciation. The transformation of glaciers into terrestrial, freshwater and (in some regions) marine ecosystems is therefore not only a biophysical process, but a societal, legal and institutional one that calls for anticipatory rather than reactive stewardship.

As the UN International Year for Glaciers' Preservation just ended, recent developments point toward how such a dynamic stewardship could be built. In line with the 1959 Antarctic Treaty system that shows how these ecosystems can be shielded from major infrastructures[52] and with the stewardship framework recently proposed[3], a motion voted positively by 97% of IUCN members during the 2025 World Conservation Congress, formally called to protect glaciers and postglacial ecosystems. This first recognition in the international agenda emphasizes the urgency to simultaneously enhance climate change mitigation and territorial protection for these ecosystems. Two recent bottom-up initiatives underscore their potential to transform policies and justice. In Switzerland, a citizen "glacier initiative" led to the 2023 Climate Protection Law, enshrining Paris Agreement objectives in the constitution, while climate litigation linking Andean glacier loss and associated risks to the emissions of a German utility[53] exemplifies how glaciers and their forelands are becoming focal points for evolving notions of climate responsibility and justice.

In addition to climate mitigation and given the imbalance we document between slowly developing ecosystems and existing or planned high-mountain infrastructures, near-term governance responses should at minimum include precautionary restrictions on new extractive, tourism or energy developments in glacier and postglacial ecosystems. Such restrictions should not be understood as rigid prohibitions on all interventions. Because glacierized and recently deglaciated landscapes can also generate hazards and may require adaptation measures, governance frameworks should explicitly distinguish between infrastructure development for economic use and scientifically justified interventions for risk reduction, ecological restoration or climate adaptation. This flexibility is essential to avoid the unintended effects of overly rigid glacier-protection laws, which may delay actions needed to reduce glacial hazards or to adapt to changing water resources[21]. Together with a strict application of existing protection frameworks, such precautionary

rules would create time and space for ecological assessment, local consultation and spatial planning. Over longer timescales, more structural reforms will be needed to develop effective, adaptive and equitably managed protection for these changing ecosystems.

As announced in 2023 in its National Strategy for Biodiversity, France has committed to rapidly put all its glacial and postglacial ecosystems under effective protection. The first concretization of this policy by the creation of a protected area (IUCN category IV) over the south of Mont-Blanc massif through a convention involving citizens, children, and economic stakeholders can serve as an example for other states and territories. In addition, the legal frameworks must be applied and strengthened as, for instance, the 2024 EU Nature Restoration Law that extended the imperative to protect the habitats recognized in 1992 as glaciers outside Natura 2000 sites. Finally, the Swiss–Italian agreement to treat glaciated borders as mobile, adjusting them as ice retreats[50], and emerging recognition of legal personality for natural entities[54], such as the Spanish laguna Mar Menor[55], complement these pathways for moving from static, object-based protection toward more dynamic, area-based stewardship adapted to changing ecosystems.

The quantitative results presented here are specific to the European Alps, where data availability, infrastructure density and governance frameworks may differ from those of other glacierized regions. Nevertheless, the underlying process—climate-driven exposure of new land that may become ecologically valuable, economically attractive and institutionally ambiguous—is not unique to the Alps[24]. Worldwide, glacier retreat has already exposed large areas, and continued warming will drastically expand them[3]. The actors, values and conflicts associated with this transition differ among regions: in some places, newly exposed land attract mining, hydropower or tourism[56]; in others, deglaciation may primarily affect water security, hazard exposure, cultural identity or spiritual relations to glacierized landscapes[57]. The Alpine case should therefore not be read as a universal template, but as an early, data-rich example of how spatial diagnoses can reveal where ecological, economic and legal claims are beginning to overlap. As shown by the weakening of the Argentinian Glacier Protection Law in April 2026, paving the way for mining developments in glacial and postglacial ecosystems, this changeover occur in regions where newly accessible minerals, water and lands already attract economical and geopolitical interests[56]. If glacier and postglacial ecosystems remain legally undefined, unregulated land-uses conflicts and irreversible ecological damages will grow in parallel with deglaciation. In this sense, the European alpine experience offers an early test case for anticipating a governance and stewardship challenge that unfolds from local to global scale. As climate change reconfigures Earth's ecosystems composition and functioning, systemic, place-sensitive and forward-looking—rather than reactive and sectorial—governance frameworks are required[1,58]. By spatially linking postglacial habitat emergence, infrastructure occupation and protection coverage, our analysis shows that deglaciation is already producing contested socio-ecological frontiers in the European Alps. Anticipatory stewardship should begin from such spatial diagnoses, while recognizing that future trajectories and appropriate policy instruments will differ across glacierized regions.

Figures

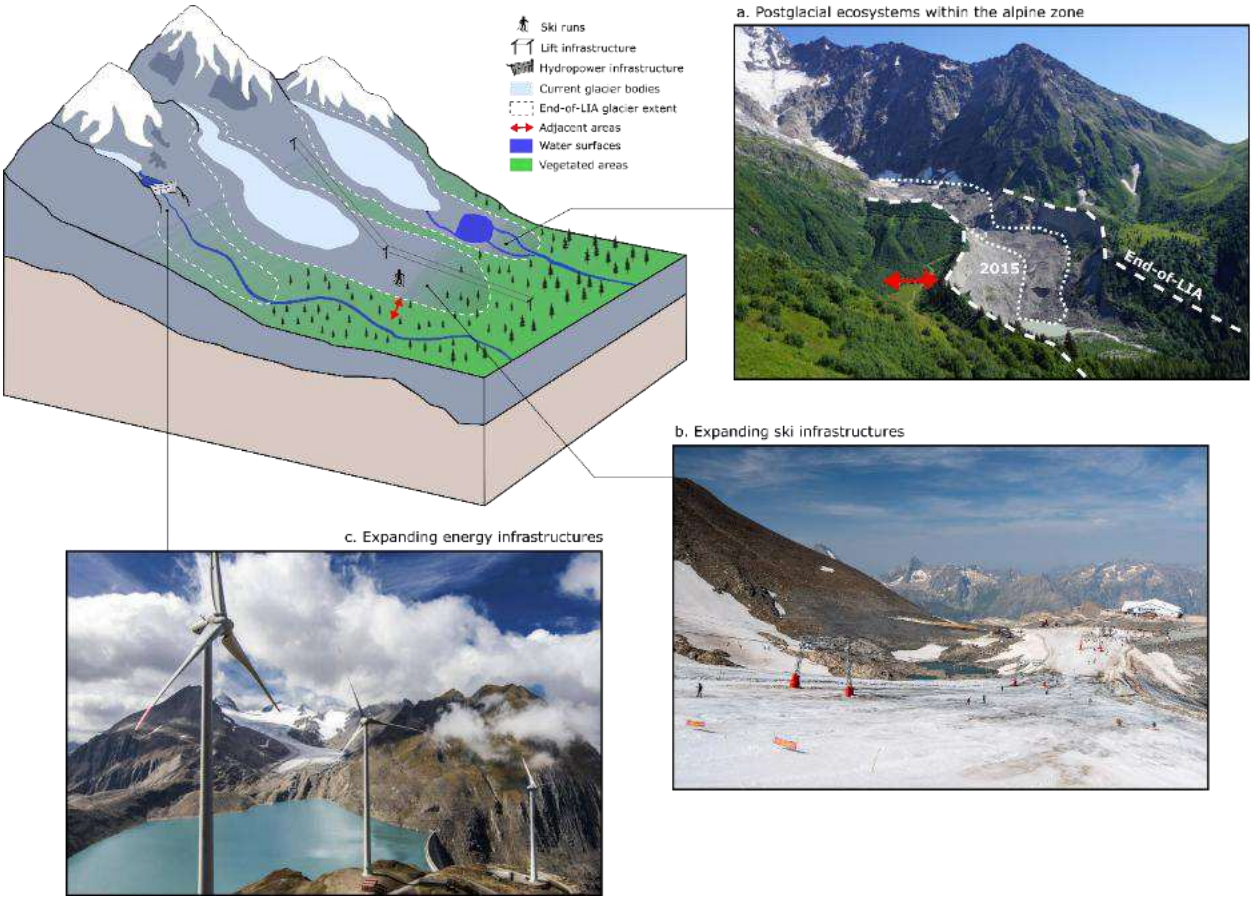


Figure 1: Illustration of glacial and postglacial areas in the Europeans Alps (a) Postglacial margin of Bionnassay glacier, Mont-Blanc, France. **(b)** Mont-de-Lans glacier, Oisans-France, with Les Deux Alpes ski resort infrastructures side by a postglacial lake. ©Thomas Pueyo **(c)** Griessee glacial and postglacial areas, Valais, Switzerland, with hydropower and wind mill infrastructures. © Olivier Maire

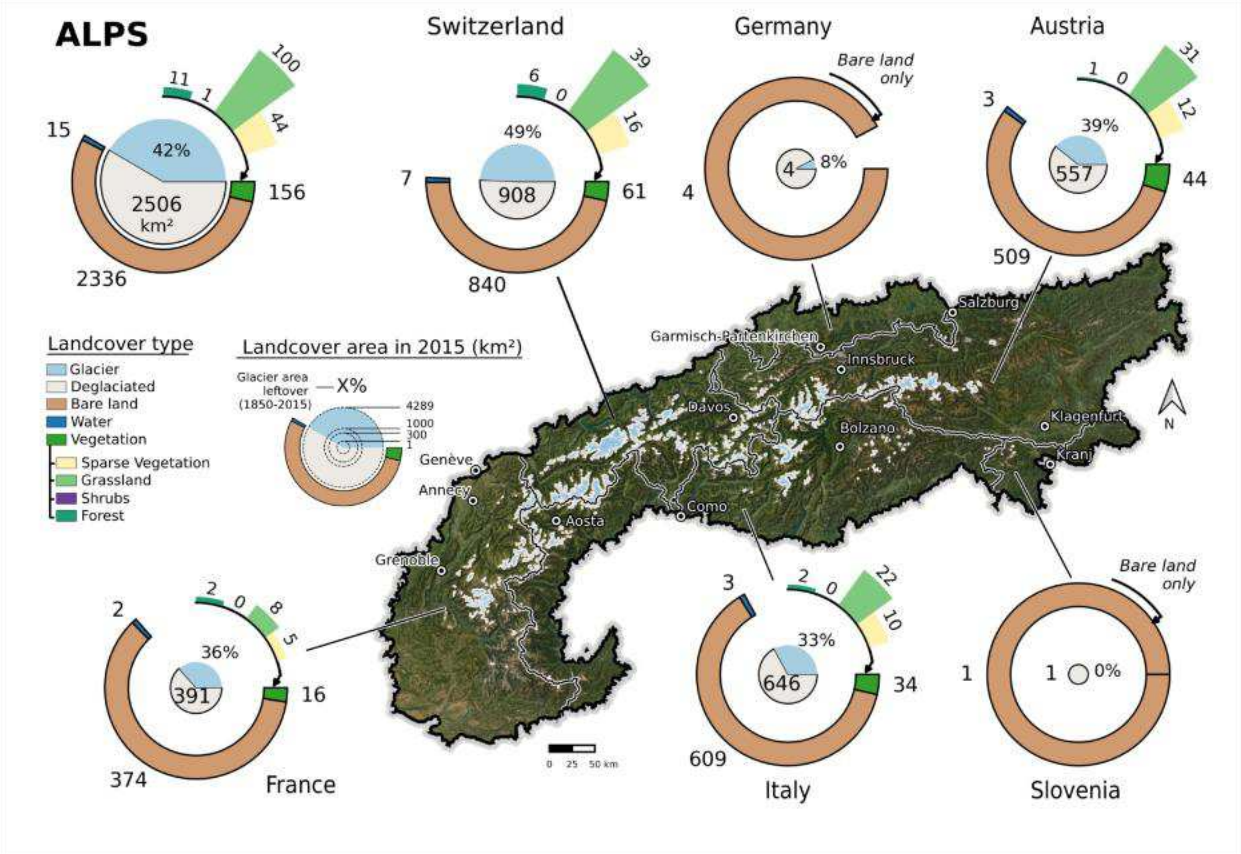


Figure 2: **Land cover of the 2015 postglacial areas in the European Alps.** Alpine and national deglaciated areas (light grey – map and inner pies) within the end-of-LIA glacier extents (size of the inner pies) along with the percentage of glacier area leftovers since then (light blue – map and inner pies). The outer pies detail the deglaciated area land cover (in square kilometer) grouped as water bodies (dark blue), bare lands (light brown) and terrestrial vegetated areas (dark green). Curved histograms give the vegetation type details, in a counterclockwise manner, between sparse vegetation (yellow), grassland (light green), shrubs (purple) and forest (dark green). Background image: © ESRI World Imagery.

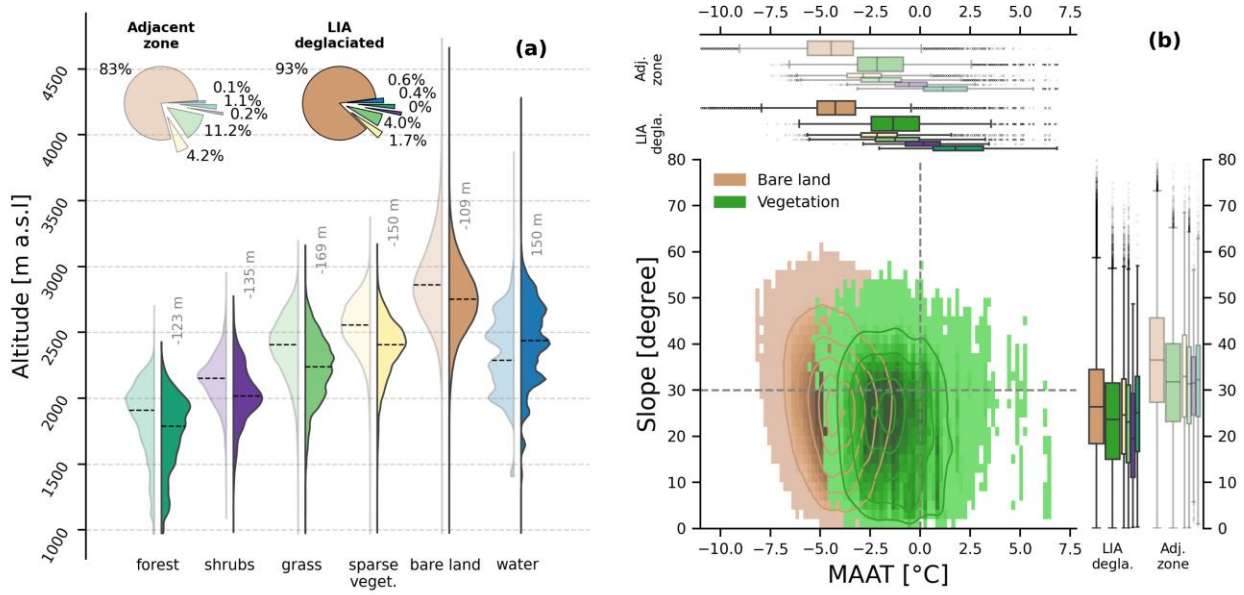


Figure 3 – Abiotic distributions of 2015 postglacial ecosystems in the European Alps (a) Land cover distribution of the 2015 postglacial areas as a function of elevation (solid colors), compared to an adjacent zone that has likely been ice-free throughout most of the Holocene (transparent colors). Horizontal dashed lines show median altitude values and vertical numbers the median altitude differences between the adjacent zone and the deglaciated areas since the end-of-LIA (LIA deglaciated). Land cover relative areas are shown on the top left pies for each respective deglaciated zone. **(b)** Bare land versus vegetated areas within the Alpine 2015 postglacial areas with respect to mean annual air temperature (MAAT) and slope. Lateral boxplots show MAAT and slope distributions for deglaciated regions within the end-of-LIA glacier extents, as well as their adjacent zones, with details on the vegetation type.

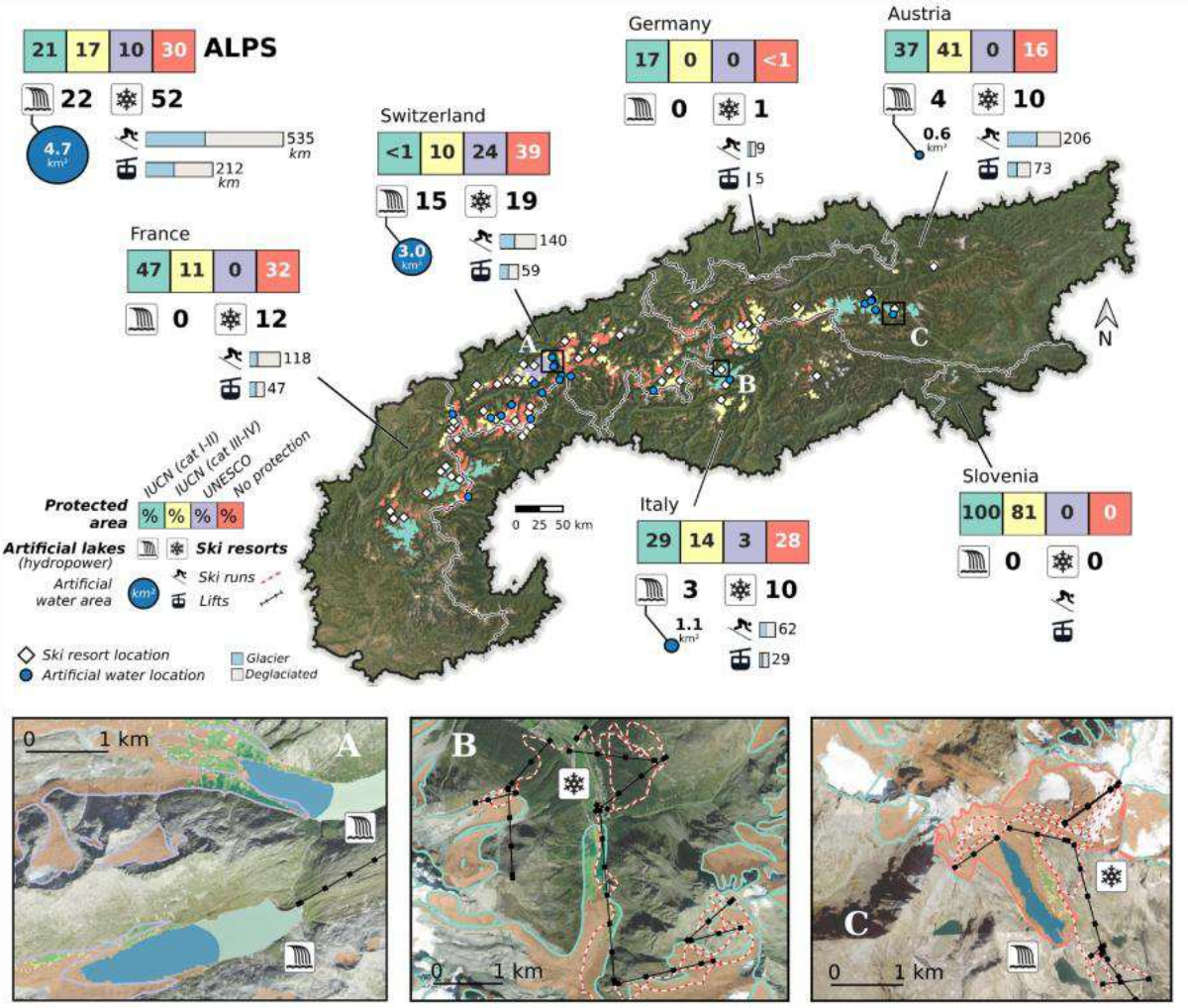


Figure 4 – Protected areas and major socio-economic activities in 2025 over the end-of-LIA glacier extents in the European Alps. **(Main map)** We show three categories of protected areas: strictly protected areas of the International Union for Conservation of Nature (IUCN) categories I and II (green), IUCN categories III and IV (yellow), and UNESCO World Heritage sites (purple); as spatial distribution (maps) and percentage of the end-of-LIA glacier extents covered (colored squares). Areas without protected status are identified in red. The number of ski resorts (white diamonds) and artificial lakes built for hydropower (blue circles) with a footprint inside the end-of-LIA glacier extents are detailed at the Alpine and national levels, with details on the resulting artificial water surface (blue circles) as well as the length of groomed ski runs and lift facilities (histograms). **(Inset maps)** Zoom in 2015 postglacial areas (colored contours) showing land cover ecosystems details, protected areas and socio-economic activities **(A)** Oberaar- and Grimselsee artificial lakes, located at the edge of the Aletsch UNESCO World Heritage site– Switzerland. **(B)** Sulden ski resort, with some infrastructures inside the Stelvio national park - Italy **(C)** Mölltaler Gletscher ski resort and Hochmurtenspeicher artificial lakes surrounded by the Hohe Tauern national park - Austria. Background image: ©ESRI Word Imagery.

References

1. Ripple, W. J. *et al.* World Scientists' Warning to Humanity: A Second Notice. *Bioscience* **67**, 1026–1028 (2017).

2. AR6 Synthesis Report: Climate Change 2023. https://www.ipcc.ch/report/ar6/syr/.

3. Bosson, J. B. *et al.* Future emergence of new ecosystems caused by glacial retreat. *Nature* **620**, 562–569 (2023).

4. Le Roy, M. *et al.* Holocene glacier variations in the Alps. *European Glacial Landscapes: The Holocene* 367–418 (2024) doi:10.1016/B978-0-323-99712-6.00018-0.

5. Zemp, M. *et al.* Community estimate of global glacier mass changes from 2000 to 2023. *Nature* https://doi.org/10.1038/s41586-024-08545-z (2025) doi:10.1038/s41586-024-08545-z.

6. Grimes, M., Carrivick, J. L., Smith, M. W. & Comber, A. J. Land cover changes across Greenland dominated by a doubling of vegetation in three decades. *Sci. Rep.* **14**, 3120 (2024).

7. Kavan, J. *et al.* New coasts emerging from the retreat of Northern Hemisphere marine-terminating glaciers in the twenty-first century. *Nature Climate Change 2025 15:5* **15**, 528–537 (2025).

8. Losapio, G. *et al.* Impacts of deglaciation on biodiversity and ecosystem function. *Nature Reviews Biodiversity* **1**, 371–385 (2025).

9. Huss, M. *et al.* Toward mountains without permanent snow and ice. *Earth's Future* vol. 5 418–435 Preprint at https://doi.org/10.1002/2016EF000514 (2017).

10. Cauvy-Fraunié, S. & Dangles, O. A global synthesis of biodiversity responses to glacier retreat. *Nat. Ecol. Evol.* **3**, 1675–1685 (2019).

11. Bollati, I. M. *et al.* Geodiversity of proglacial areas and implications for geosystem services: A review. *Geomorphology* **421**, 108517 (2023).

12. Milner, A. M. *et al.* Glacier shrinkage driving global changes in downstream systems. *Proceedings of the National Academy of Sciences* **114**, 9770–9778 (2017).

13. Motion 017 | iucncongress2025.org. https://iucncongress2025.org/assembly/motions/motion/017.

14. Aska, B. *et al.* Mining, biodiversity and social conflict in the renewable energy transition. *Nature Reviews Biodiversity* **1**, 597–614 (2025).

15. Kellner, E. & Brunner, M. I. Reservoir Governance in World's Water Towers Needs to Anticipate Multi-purpose Use. *Earths Future* **9**, (2021).

16. Ausserladscheider, V. Decoupling climate change: winter tourism and the maintenance of regional growth. *New Political Economy* **29**, 693–708 (2024).

17. Ficetola, G. F. *et al.* The development of terrestrial ecosystems emerging after glacier retreat. *Nature* https://doi.org/10.1038/s41586-024-07778-2 (2024)

18. Zimmer, A., Beach, T., Klein, J. A. & Recharte Bullard, J. The need for stewardship of lands exposed by deglaciation from climate change. *Wiley Interdisciplinary Reviews: Climate Change*,13 (2), e753 (2022).

19. Gagné, K., Rasmussen, M. B. & Orlove, B. Glaciers and society: attributions, perceptions, and valuations. *WIREs Climate Change,* 5:793-808 (2014)

20. Allison, E. A. The spiritual significance of glaciers in an age of climate change. WIREs Climate Change, 6:493-508. (2015)

21. Anacona, P. I. et al. Glacier protection laws : potential conflicts in managing glacial hazards and adapting to climate change. Ambio, 47:835-845. (2018)

22. Schuster, L. *et al.* Irreversible glacier change and trough water for centuries after overshooting 1.5 °C. *Nature Climate Change 2025 15:6* **15**, 634–641 (2025).

23. Reinthaler, J. & Paul, F. Reconstructed glacier area and volume changes in the European Alps since the Little Ice Age. *Cryosphere* **19**, 753–767 (2025).

24. Van Tricht, L. *et al.* Peak glacier extinction in the mid-twenty-first century. *Nat. Clim. Chang.* https://doi.org/10.1038/s41558-025-02513-9 (2025) doi:10.1038/s41558-025-02513-9.

25. Mu, H. *et al.* A global record of annual terrestrial Human Footprint dataset from 2000 to 2018. *Sci. Data* **9**, (2022).

26. Paul, F. *et al.* Glacier shrinkage in the Alps continues unabated as revealed by a new glacier inventory from Sentinel-2. *Earth Syst. Sci. Data* **12**, 1805–1821 (2020).

27. Bayle, A. *et al.* Sensitivity of Landsat NDVI to subpixel vegetation and topographic components in glacier forefields: assessment from high-resolution multispectral UAV imagery. https://doi.org/10.1117/1.JRS.15.044508ï (2021) doi:10.1117/1.JRS.15.044508ï.

28. Bayle, A. *et al.* Local environmental context drives heterogeneity of early succession dynamics in alpine glacier forefields. https://doi.org/10.5194/egusphere-2022-1164 (2023) doi:10.5194/egusphere-2022-1164.

29. Shugar, D. H. *et al.* Rapid worldwide growth of glacial lakes since 1990. *Nat. Clim. Chang.* **10**, 939–945 (2020).

30. Eichel, J. Vegetation Succession and Biogeomorphic Interactions in Glacier Forelands. in 327–349 (2019). doi:10.1007/978-3-319-94184-4_19.

31. Schaller, S. *et al.* Postglacial evolution of Lake Constance: sedimentological and geochemical evidence from a deep-basin sediment core. *Swiss Journal of Geosciences 2022 115:1* **115**, 7- (2022).

32. Wojcik, R., Eichel, J., Bradley, J. A. & Benning, L. G. How allogenic factors affect succession in glacier forefields. *Earth. Sci. Rev.* **218**, 103642 (2021).

33. Eichel, J., Draebing, D., Winkler, S., & Meyer, N. Similar vegetation-geomorphic disturbance feedbacks shape unstable glacier forelands across mountain regions. Ecosphere, 14(2), e4404 (2023)

34. Gobbi, M. *et al.* Vanishing permanent glaciers: climate change is threatening a European Union habitat (Code 8340) and its poorly known biodiversity. *Biodiversity and Conservation 2021 30:7* **30**, 2267–2276 (2021).

35. Wilkes, M. A. *et al.* Glacier retreat reorganizes river habitats leaving refugia for Alpine invertebrate biodiversity poorly protected. *Nature Ecology & Evolution 2023 7:6* **7**, 841–851 (2023).

36. Velasquez Casallas, L. M., Khelidj, N., Morán-Ordóñez, A. & Losapio, G. Global impacts of glacier retreat on ecosystem services provided by soil and vegetation in mountain Regions: A literature review. *Ecosyst. Serv.* **73**, 101730 (2025).

37. Jiang, F., Fatichi, S., Losapio, G. & Peleg, N. Future glacier retreat and forest expansion in the Swiss Alps provide limited benefits for carbon sinks. *Agric. For. Meteorol.* **372**, (2025).

38. Khedim, N. *et al.* Topsoil organic matter build-up in glacier forelands around the world. *Glob. Chang. Biol.* **27**, 1662–1677 (2021).

39. Troxler, P., Roller, M. & Bandi Tanner, M. The development of ski areas and its relation to the Alpine economy in Switzerland. *Swiss Journal of Economics and Statistics 2024 160:1* **160**, 10- (2024).

40. Duvillard, P. A., Ravanel, L., Marcer, M. & Schoeneich, P. Recent evolution of damage to infrastructure on permafrost in the French Alps. *Regional Environmental Change 2019 19:5* **19**, 1281–1293 (2019).

41. Spitale, D., Angeli, N., Lencioni, V., Tolotti, M. & Cantonati, M. Comparison between natural and impacted Alpine lakes six years after hydropower exploitation has ceased. *Biologia 2015 70:12* **70**, 1597–1605 (2015).

42. Explore the World's Protected Areas. https://www.protectedplanet.net/en/thematic-areas/wdpa?tab=WDPA.

43. Europe′s environment and climate: knowledge for resilience, prosperity and sustainability Europe′s environment. https://doi.org/10.2800/3817344 (2025) doi:10.2800/3817344.

44. Bosson, J. B., Huss, M. & Osipova, E. Disappearing World Heritage Glaciers as a Keystone of Nature Conservation in a Changing Climate. *Earths Future* **7**, 469–479 (2019).

45. Bütler, M. & 66, G. Glaciers − Objects of Law and International Treaties. http://www.antarctica.ac.uk/About_Antarctica/Treaty/index.html; (2007).

46. Pope, A. Glacier or not? The importance of nuance in definitions of vanishing glaciers. *Ann. Glaciol.* **66**, e32 (2025).

47. Yolka, P. Les glaciers de montagne à l'épreuve du réchauffement climatique (une protection juridique à inventer). *Revue juridique de l'environnement* **45**, 559–568.

48. Held, J., Neuerer, F. & Schmid, H. Tiroler Naturschutzgesetz 2005. https://www.verlagoesterreich.at/tnschg-2005/99.105005-9783704679833 (2005).

49. Louvin, Roberto. Diritto glaciale e post-glaciale. https://arts.units.it/handle/11368/3119998 (2025).

50. Billet, P. Considérations juridiques sur le statut des espaces post-glaciaires. *Revista General de Derecho Público Comparado - ISSN 1988-5091* (2024).

51. Carvalho Resende, T. *et al.* World Heritage Glaciers: Sentinels of Climate Change. 1–34 (2022) doi:10.3929/ETHZ-B-000578916.

52. Kubiszewski, I. *et al.* Cascading tipping points of Antarctica and the Southern Ocean. *Ambio 2024 54:4* **54**, 642–659 (2024).

53. Nogrady, B. Justice on the horizon. *Nature* **644, S1**, (2025).

54. Gilbert, J. Creating Synergies between International Law and Rights of Nature. *Transnational Environmental Law* **12**, 671–692 (2023).

55. Rehnstrom, S. & Rehnstrom, S. Rights of Nature in Europe: the Mar Menor and the Future of Ecocentric Environmental Protection. *Journal for European Environmental & Planning Law* **22**, 346–363 (2025).

56. Castelvecchi, D. US scientists push back as Trump eyes Greenland. *Nature* https://doi.org/10.1038/D41586-026-00068-Z (2026) doi:10.1038/D41586-026-00068-Z.

57. Veh, G., & al. Progressively smaller glacier lake outburst floods despite worldwide growth in lake area. Nature Water, 3, 271-283. (2025)

58. Pörtner, H.-O. *et al.* Scientific outcome of the IPBES-IPCC co-sponsored workshop on biodiversity and climate change. https://doi.org/10.5281/ZENODO.5101125 doi:10.5281/ZENODO.5101125.

Methods

Definition of postglacial areas

Postglacial areas[3] are today deglaciated regions located between contemporary glacier extents and its boundaries at the end of the Little Ice Age (LIA, around 1850 in the Alps[59]). To identify these regions in the Europeans Alps, we intersected end-of-LIA glacier outlines with the latest current (2015) spatially consistent glacier extents[26]. We used the end-of-LIA glacier outlines from reference[23] everywhere but France, where we used refined work[60] to integrate unexplored regions and missing small glaciers. End-of-LIA datasets rely on expert interpretation of geomorphological traces (e.g., trimlines, moraines) visible on high-resolution aerial and satellite images, whereas current glacier extents rely on automatic classification of 2015 Sentinel-2 satellite images and extensive manual post-processing. We only retained 2015 glacier areas that lied within end-of-LIA glacier extents, excluding 23 km² of ice-covered area, mainly in Switzerland and Italy, due to slight misalignments and/or the presence of small glaciers not included in the end-of-LIA glacier mapping. We removed resulting polygons smaller than 0.01 km², which accounted for an additional 0.4 km². The resulting glacier outlines define an end-of-LIA glacier extent of 4,289 km² across the European Alps. Of this, 1,783 km² remained ice-covered in 2015, corresponding to a net deglaciated area of 2,506 km², or 58%. To compare the distribution of land cover classes on postglacial areas to adjacent areas, likely ice-free during most of the Holocene (~11.000 years ago[4]), we defined a 200-m buffer band around each end-of-LIA glacier outline, from which we removed 2015 glacierized and postglacial areas, as well as those whose elevation was outside the altitudinal range of the given end-of-LIA glacier outline. This way we obtained a 2450 km² area, of the same altitudinal range than the 2506 km² of postglacial lands, with similar current climatic parameters, on which we perform the same land cover mapping as for postglacial areas.

It is important to notice that Alpine glaciers have strongly retreated between 2015 and 2025, due to an acceleration of mass and area loss with several record years[61]. Our land cover mapping is therefore not fully accounting for the present state. The successive glacier inventories in Switzerland point out an acceleration of ice melt and a value of annual area loss of 1,7% between 2016 and 2023[62]. Assuming this as is representative for the Alpine glacier loss rate, we may assume that another 250 km² has transformed into deglaciated terrain between 2015 and 2025, i.e., ~10% of the postglacial areas accounted here. These areas are not accounted for in our delineation of postglacial areas but treated as glacierized areas in all the study. However, our main objective being to investigate long-term changes in land cover since ~1850, from glaciers to new ecosystems, this surface can be neglected on this timescale. Nevertheless, postglacial land cover areas given here are minimum values.

Land cover mapping of postglacial ecosystems

Land cover classes definition

To capture aspects of the ecological diversity and functional characteristics of postglacial landscapes, we defined a set of land cover classes representative of the main habitats currently present within and around the end-of-LIA glacier extents across the European Alps. The classification aims to distinguish between rocky and vegetated dominated surfaces, early- and late-successional vegetation, and aquatic systems. We selected six primary land cover classes, chosen for their ecological relevance, detectability via remote

sensing, and comparability with existing land cover inventories: (1) Bare lands, represent rocky and sedimentary dominated surfaces including glacial till, moraines, bedrocks, as well as coarse sediments of non-glaciogenic origin, hosting a large diversity of micro-organism as well as some pioneer vegetation. These areas dominate early-stage postglacial terrain and serve as the initial substrate for primary succession[30]. (2) Sparse vegetation, includes early successional vegetation with low canopy cover and limited spectral greenness. It includes mosses, lichens, and scattered herbaceous species. (3) Grasslands, are herbaceous-dominated communities with moderate to high vegetative cover, representing later stages of succession or stable alpine meadows. This class plays a central role in carbon sequestration and slope stabilization[62]. (4) Shrublands include woody perennial vegetation below forest height thresholds. In the Alps, this includes communities dominated by Ericaceae, Juniperus, or Rhododendron, typically occupying intermediate altitudes and ecotones. Because our classification relies on anthocyanin pigment accumulation (see 'Remote sensing data'), land cover classified as shrublands are expected to be mostly Ericaceous dominated shrublands. (5) Forests represent continuous woody vegetation forming closed canopies, including coniferous, deciduous, or mixed stands. No separation between those is made within this class. (6) Natural and artificial lakes are surface water bodies formed in glacial depressions (e.g., moraine or bedrock-dammed lakes, kettle lakes) after glacier retreat. It also includes dammed reservoirs and regulated lakes associated with hydropower infrastructures. Since no surface threshold and/or shape filtering are applied on water bodies detection, potential postglacial rivers can be accounted for as lakes but found to be very limited (see 'Water mapping'). Water bodies such as alluvial planes, keys to plant colonization in postglacial areas[64], even though sometimes as large as lakes[65], are hardly detected with our method due to their high temporal and spatial variations.

Remote sensing data

Despite numerous land cover products available at global[66,67,68,69] and regional scales[70,71,72,73] with spatial resolution of 10-30 m, none have been tuned to perform well on mountainous areas, and even less in postglacial areas. Most of the time focusing on low elevation terrain, impervious regions and/or croplands, these products ignore specific high-mountainous land cover classes and/or show poor mapping quality at glacier margins[74]. We here choose to build our own land cover mapping of postglacial areas in this sense. Our analysis relies on remote sensing data from Sentinel-2A and Sentinel-2B Copernicus Earth observation satellite missions. The 5-day revisit time available since March 2017, combined with a 10-20 m spatial resolution, enables to detect patchy and heterogeneous plant canopies distributed across topographically complex terrain[75] such as postglacial areas. In addition, Sentinel-2 red-edge sensors improved determination of pigment seasonal variability in plants, enhancing mountain vegetation discrimination[76]. For terrestrial land cover mapping, we computed two spectral indices: Normalized Anthocyanin Reflectance Index (NARI) and Normalized Chlorophyll Reflectance Index (NCRI), which are both normalized adaptations of three-band models[77]. NARI and NCRI are sensitive to plant canopy anthocyanin and chlorophyll content, respectively, found to outperform popular global land cover products when computed over specific phenological windows. To reduce sensitivity to inter-annual phenological variability and observation artefacts, we calculated monthly median composites for each spectral index over the 2017–2023 period. For each of the three periods: 15 July–15 August, 15 August–15 September, and 15 September–15 October, the median value was computed from all valid Sentinel-2 observations available during that month across the seven-year period. The resulting predictors therefore represent recurrent seasonal spectral behavior over the recent observation period, rather than year-specific conditions. This multi-year compositing strategy

was used to stabilize pigment-sensitive indices such as NARI and NCRI, whose values can vary among years in response to temperature, radiation and snowmelt timing. We used three fixed seasonal periods across the Alpine domain to provide a standardized spectral-temporal reference for all pixels and land-cover classes. These periods were not intended to match the local peak growing season at every elevation or aspect. Instead, they were selected to capture complementary phases of alpine vegetation phenology, from summer chlorophyll-related greenness to late-season anthocyanin-related and senescence signals. Using the same three periods across the study area allows spectral responses to be compared under a common seasonal framework. Although phenological timing varies with elevation, aspect and local snowmelt conditions, this variation also contributes to the spectral-temporal signal used to discriminate broad land-cover classes. Resulting indices were used as predictive variables, i.e., six variables noted NARI $_{7\text{-}8\text{-}9}$ and NCRI $_{7\text{-}8\text{-}9}$, in the random forest classification model to map terrestrial land cover (see 'Terrestrial land cover classification'). For water surface mapping, we computed the median value of the Normalized Difference Water Index (NDWI)[78] over the same time window, optimizing the ice-free period of glacial lakes. All spectral bands were obtained at Surface Reflectance (SR) level from Google Earth Engine (GEE)[79] 'Copernicus/S2_SR' dataset including atmospheric correction from Sen2Cor[80]. We post-processed all images with the Python 'eemont' module[81], filtering out images with more than 60% cloud cover fraction and masking cloud (including cirrus) and shadows with probability threshold greater than 0.6.

Training datasets

We used a random forest algorithm approach to map land cover classes (1)-(3)-(4)-(5). This approach consists of training a computational model with "ground-truth" observations to predict outputs (here land cover) through predictive variables. This section describes how we elaborated "ground-truth" observations, also called training dataset, i.e., geo-referenced points of land cover classes (1)-(3)-(4)-(5) across the European Alps. Such high-quality training datasets remain limited for postglacial areas. Indeed, widely used global datasets often lack adequate representation in high-mountainous regions, critical for classes such as shrublands and bare rock[82,83,84]. To address this, we constructed a customized training dataset for the European Alps, combining and augmenting existing sources with visual photointerpretation of high-resolution aerial and satellite imagery. We first extracted data from the Global Land Cover Estimation (GLanCE) dataset[84], focusing on all points within the Alpine Convention region located above 1000 m a.s.l. consistent with the lower bounds of the LIA glacier extent. GLanCE offers several advantages over its foundational dataset, LUCAS[83], including harmonized land cover classes, additional confidence filtering, and extra visual validation. From GLanCE, we retained only classes relevant to our study: bare rock, grassland, and forest (encompassing evergreen, deciduous, and mixed stands). Due to limited Ericaceae-dominated shrublands representation in GLanCE, we extended an existing dataset[76] across the broader Alpine region, with special care to balance representation across countries despite the natural spatial clustering of shrubland patches. To enhance classification quality, we excluded shrublands points that did not exceed NARI = 0.3 in any of the July, August or September composites (i.e. NARI7, NARI8 and NARI9 all ≤ 0.3) as they were identified as potentially ambiguous, because they often corresponded to shadows, mixed pixels, senescent or sparse vegetation, or mislabeled non-vegetated surfaces. For Switzerland, which is not covered by LUCAS or GLanCE, we relied on a national 25 m-resolution land cover map[85] derived from the Swiss National Base Maps and Land Use Statistics using aerial photointerpretation and downscaling through a nearest-neighbor and expert-based system. From this map, we selected pixels above 1000 m a.s.l. falling into relevant classes (bare lands, grassland, forest) and randomly sampled ~1000 points

per class. All selected pixels were visually checked by two co-authors with expertise in remote sensing and alpine environments using Google Earth and ESRI World Imagery. During this quality-control step, we removed points affected by obvious interpretation or geolocation errors, including points falling on cast shadows, steep cliffs or ridges faces with strong topographic illumination effects, snow or ice remnants, infrastructure, mixed pixels located at class boundaries, or pixels whose visual land cover clearly contradicted the original label. Examples of retained and rejected training points are provided in Fig. S1 to illustrate some of the criteria used during manual verification. Because the mapped classes are broad land-cover categories rather than species-level or community-level units, most labels are visually interpretable in high-resolution imagery. The main objective of the training dataset was therefore not only to verify that each point corresponded to its assigned class, but also to capture the spectral variability encountered within each class across the European Alps. For instance, the forest class includes coniferous, deciduous and mixed stands across different elevations and illumination contexts, while the bare-land class includes bedrock, moraines, glacial till and coarse sediments. We therefore retained training points spanning this variability, while removing points affected by clear labelling errors or ambiguous mixed-pixel conditions. Lastly, to supplement the bare rock class underrepresentation in GLanCE (only one point met our selection), we manually constructed an independent training dataset of bare lands points through direct visual photointerpretation for all Alpine countries except Switzerland (already covered), with special care again to balance representation across countries and drawn from terrain above 1000 m a.s.l. Overall, we obtained 9384 training points, distributed as follows: 2776, 2216, 2048, 2344 samples for bare lands, grasslands, shrublands, and forest respectively (Fig S2).

Terrestrial land cover classification, validation and uncertainties

We used GEE supervised random forest (RF) algorithm to build a classification model for the terrestrial land cover (1)-(3)-(4)-(5). We computed our final RF model based on a spatial-split approach using the six predictive variables $NARI_{7\text{-}8\text{-}9}$ and $NCRI_{7\text{-}8\text{-}9}$ on the training dataset locations (see 'Training dataset') (Fig S3). We first tuned the RF number of trees to 200 based on the "out of bag error" estimate and chose a number of variables per split of 3, i.e., higher than the default square root of the number of predictive variables, hence limiting overfitting. We have not tuned more parameters since there is no performance gain in doing so[86]. We used a 4-fold spatial-split pattern to train and validate our model (Fig S2). For each fold, one spatial block was withheld as an independent test set, while the model was trained on the remaining three blocks using the same RF parameters. Accuracy metrics and the confusion matrix reported in Fig. S4 were computed from the aggregation of these out-of-fold predictions (Fig. S5), not from predictions on the training data. This spatial validation design was chosen to reduce data leakage and overoptimistic accuracy estimates caused by spatial autocorrelation, which can occur with random train–test splits in remote-sensing classification[87,88]. We found similar performances for all RF models and chose to follow an ensemble learning approach. Because each fold was spatially withheld, this validation also tested whether the classifier could generalize across Alpine subregions with different species composition, illumination conditions and spectral expressions of the same broad land-cover classes. We combined the outputs of the 4 random forests to estimate the final land cover classification, i.e., by averaging the output probabilities per land cover class of the four models, without weights[89] and estimated our final model accuracy based on the combined confusion matrix (Fig S4). Area uncertainties were estimated from conformal predictive sets applied to the ensemble probabilities. Class (2)-sparse vegetation classification has not been performed through the RF process but based on the final model output probabilities of the land cover classes (1)-bare

lands and (3)-grasslands. It has been motivated by the observation of a high number of pixels with similar output probabilities for these two latter classes. We thus re-classified pixels to class (2) when their predictive set (see below) contained only classes (1) and (3). Such pixels appeared clearly to fall between the classes (1) and (3) in the (NARI $_{7\text{-}8\text{-}9}$ / NCRI $_{7\text{-}8\text{-}9}$) space (Fig S3), consistent with a continuum of vegetation cover in partially colonized postglacial terrain. We explored whether analogous mixed classes could be derived for bare-land–shrubland and bare-land–forest transitions using the same probability-overlap logic. These combinations were almost absent in the RF probability space, with only three pixels showing comparable bare-land/forest overlap and four pixels showing comparable bare-land/shrubland overlap across the study area. We therefore restricted the derived sparse-vegetation class to the bare-land–grassland continuum, which was the only substantial mixed end-member transition detected by the model. However, this should not be interpreted as evidence that sparse woody colonization or bare–shrub and bare–forest transitions are absent in the field. Rather, these transitions are not reliably resolved by our Sentinel-2 phenological feature space and broad end-member training strategy at 20 m resolution. Consequently, the sparse-vegetation class should be interpreted as a conservative estimate of the dominant bare-land–herbaceous vegetation transition, while sparse shrubland or early woody colonization may be under-detected or represented within bare land, grassland or sparse vegetation.

We used conformal statistics[90,91] to estimate terrestrial land cover uncertainties. This theory allows pixel-level uncertainty quantification for categorized data with relatively little computational power and straightforward implementation for any algorithm that outputs class probabilities[92]. For each Sentinel-2 pixel, we derived what is called a 'predictive set'. This predictive set corresponds to the ensemble of land cover classes for which the true class is likely to be one of those at a certain confidence level C. In practice, the predictive set is derived based on the conformal scores of the training dataset, i.e., the 1-C quantile of the model probabilities of the true class of the training dataset. A given pixel is considered uncertain at the level C when the size of its predictive set is different than one, i.e., there is more than one land cover class with higher probability than the conformal score (multiple classification possible), or there is no land cover class at all with higher probability than the conformal score (no classification with high enough confidence level). We here chose to derive uncertainties at the 95% confidence level. From such an uncertainty map (Fig S6), we derived land cover area uncertainties as follow: negative uncertainty of a given land cover class corresponds to the pixels classified as such that have a predictive set of size different than one; positive uncertainty corresponds to the pixels not classified as such that contain the given land cover class in their predictive set. Land cover class (2)-sparse vegetation being defined from the other classes' probabilities, its area uncertainties cannot be directly estimated through this procedure since we do not have conformal scores for this class. The area uncertainty reported for each terrestrial land-cover class was obtained by summing the surface of pixels whose conformal predictive set indicated possible class reassignment. For a given class, the negative uncertainty corresponds to pixels classified as that class, but whose predictive set contained either multiple possible classes or no class at the chosen confidence level. The positive uncertainty corresponds to pixels assigned to another class, but whose predictive set included the focal class. These pixel areas were then aggregated at Alpine and national scales and converted into percentages using the corresponding deglaciated or vegetated-area denominator. Uncertainty in percentages is not shown to keep results readable. This procedure of terrestrial classification and estimation of associated uncertainties has been performed simultaneously on postglacial areas and their adjacent zone. The resulting land cover map is representative of the year 2020.

High-resolution sub-pixel characterization of land-cover classes

To characterize the sub-pixel composition of the 20 m land-cover classes, we compared our Sentinel-2 classification with independent high-resolution vegetation and canopy-structure data over the Mont-Blanc massif. We used a 20 cm NDVI raster derived from infrared aerial orthophotography (©IGN BDORTHO IRC 20cm from 2023) and a 50 cm canopy-height model derived from airborne LiDAR (©LiDAR HD IGN from 2023). These datasets were used as an independent high-resolution benchmark to assess how the 20 m land-cover classes relate to sub-pixel greenness and vegetation structure (Fig. S7). NDVI raster was reprojected to 50cm spatial resolution based on LiDAR HD grid. Both 50 cm rasters were projected, cropped and aligned to the 20 m land-cover grid. For each 20 m land-cover pixel, we aggregated all underlying 50 cm pixels and calculated four summary metrics: mean NDVI, NDVI variance, mean canopy height and canopy-height variance. Mean NDVI was used as an indicator of average sub-pixel vegetation signal, while NDVI variance was used to characterize within-pixel heterogeneity in greenness. Mean canopy height and canopy-height variance were used to assess whether mapped classes differed in vertical vegetation structure and whether sparse-vegetation pixels corresponded to low-stature vegetation rather than unresolved woody vegetation. This analysis was used to characterize the physical meaning of the mapped classes at sub-pixel scale, with particular attention to the bare-land–sparse-vegetation–grassland transition (Fig. S8). Only 5 pixels of shrubland were identified in our Mont-Blanc massif dataset so it was not included in the analysis. The transition from bare land to forest was found to be coherent based on mean NDVI and Canopy Height values with continuous gradients of mean NDVI, and canopy height superior to 0 mostly for Forested pixels (Fig. S8a-c). Some grasslands were found to have Canopy Height superior to 0 which might indicate contamination of grasslands pixels by very sparse tree. Variance in canopy height was high for Forested pixels only and nearly absent for other classes. NDVI variance was the highest for grassland and sparse vegetation which confirms the intermediate position of sparse vegetation between grassland and bare land. For grassland, the high variance in NDVI might indicate the presence of sparse trees contamination (Fig. S8d-f). Because the high-resolution comparison is restricted to the Mont-Blanc massif, we interpret it as a regional sub-pixel characterization and independent high-resolution benchmark, rather than as a complete external validation of the Alpine-wide land-cover map. It was therefore used to clarify the interpretation and limitations of the Sentinel-2 classes, especially the fact that pixels classified as bare land may still contain unresolved pioneer vegetation below the 20 m mapping resolution.

To further characterize fine-scale greenness within the low-vegetation classes, we also calculated the proportion of positive-NDVI 50 cm cells within each 20 m land-cover pixel. The 50 cm NDVI raster was converted to a binary layer in which cells with NDVI > 0 were assigned a value of 1 and cells with NDVI ≤ 0 were assigned a value of 0. This binary layer was then aggregated to the 20 m land-cover grid by averaging all 50 cm cells falling within each 20 m pixel. Because the input layer is binary, the resulting value corresponds to the proportion of 50 cm cells with positive NDVI within each 20 m pixel. This analysis was applied to pixels classified as bare land, sparse vegetation and grassland, and was used to quantify the fine-scale greenness signal contained within each class. We then calculated, for each class, both the distribution of positive-NDVI fractions and the proportion of 20 m pixels containing at least one positive-NDVI 50 cm cell. This provided an additional test of whether bare land, sparse vegetation and grassland form an ordered sub-pixel greenness continuum. The analysis showed that 12.8% of pixels classified as bare land contained at least one positive-NDVI 50 cm cell, generally in very low proportions, whereas positive-NDVI cells were present in 96.5% of sparse-vegetation pixels and 97.7% of grassland pixels. Sparse vegetation also occupied an intermediate position between bare land and grassland in the distribution of positive-NDVI fractions, with a mean positive-NDVI fraction of 17.3% [9–28%], compared with 45%

[23–67%] for grassland (Fig. S9). This supports the interpretation of bare land, sparse vegetation and grassland as a landscape-scale continuum of increasing vegetation cover, while confirming that pixels classified as bare land can still contain very sparse sub-pixel vegetation below the 20 m mapping resolution.

Water mapping, validation and error assessment

Water surface detection by remote sensing is a very active field that produced a flourishment of methods[93], from historical index thresholds[94,29] to more complex ones such as supervised algorithms[95,96], with an increased use of multi-sensors[92]. Here we used a combination of optical remote sensing reflectance and topographic indexes to map water surface over deglaciated areas inside the end-of-LIA glacier outlines as well as the adjacent zones. Topographic filtering allows us to remove implausible detections (e.g., high slope, ridge tops), and the exclusion of glacierized areas prevents numerous false detections from temporary summer glacial streams. We used the Normalized Difference Water Index (NDWI)[78] computed from Sentinel-2 Surface Reflectance product averaged over snow-free period (July 15th to October 15th) between 2017 and 2023 (included) and applied a slope filtering based on Copernicus EU-DEM at 30 m (see 'Climate and topographic data'). To choose both indexes' thresholds, we compared the resulting water mapping for various thresholds to a validation dataset[98] over the French area. This dataset contains all water surfaces identified above 1500 m a.s.l., without size limitation, from 2022 national ortho imagery interpretation. To assess the sensitivity of the mapped water surface to the NDWI threshold, we repeated the water classification using NDWI thresholds ranging from 0.1 to 0.2, while keeping the slope threshold fixed at 20°. This range encompasses plausible values commonly used for NDWI-based surface-water detection. Thresholds below this range produced numerous false positives, especially over wet snow, shaded terrain and lake margins, whereas higher thresholds increasingly restricted detections to larger or optically darker water bodies and omitted small or shallow lakes. Over the French validation area, varying the NDWI threshold within this range changed the mapped water surface by approximately ±0.5 km² around the selected threshold (Fig. S10). Based on this comparison, we chose $NDWI_{thresh}$= 0.15 and $slope_{thresh}$= 20 to maximize detection performance while limiting false detection. Indeed, weaker thresholds increased water surface detection and so the associated completeness performance, but this is mostly due to limited Sentinel-2 resolution leading to additional water detection on individual lake ridges (wrongly mapped). We visually validated ~80% of the mapped lakes to ensure reliability, confirmed by very good performance results for lakes larger than 0.1 ha (equivalent to about two Sentinel-2 pixels area) with 96%-count and 80%-surface completeness (Fig S11). Other national water mappings of glacial lakes in Switzerland[99] and Austria[100] also show very good agreement with our results, i.e., 6.22+/-0.25 km^2 versus 6.7 km^2 (our result, Switzerland) and 2.93 km^2 versus 3.1 km^2 (our result, Austria). It is important to note that we excluded the 2015 glacierized area from the water mapping and thus missed the last 10-years of lakes evolution in postglacial areas. From the French validation dataset, we estimate the corresponding missing surface to ~10% (~0.2 km² in France).

Climate and topographic data

To characterize the abiotic conditions shaping postglacial ecosystems development, we extracted climate and topographic variables across the full extent of the end-of-LIA glacier outlines, as well as for the adjacent zone. Climate data were obtained from the Climatologies at High Resolution for the Earth's Land Surface Areas (CHELSA) v2.1 dataset[101] which provides high-resolution (~1 km) climatological variables for global land areas. CHELSA is based on statistical downscaling of ERA5 reanalysis data, corrected using

orographic predictors and station observations, and is particularly suited for complex topographic regions such as the European Alps. Among available variables, we selected Mean Annual Air Temperature (MAAT) as the primary climatic driver of vegetation establishment and succession. We used the 1981–2010 climatological reference period to represent average thermal conditions of the recent period in which postglacial ecosystems have developed.

Topographic variables were derived from the Copernicus Digital Elevation Model (GLO-30 DEM)[102], available on GEE with a native resolution of 30 m. From this dataset, we computed the following terrain metrics on GEE platform: (i) Elevation (m a.s.l.); (ii) Slope (degrees); and (iii) Aspect. All topographic layers were resampled to a 20 m resolution to align with the satellite-derived land cover data. Topographic data were primarily used to investigate constraints on vegetation development (e.g., slope thresholds for colonization) and to filter false positives in water detection in steep or shadowed zones.

Ecosystemic services

This section describes how we estimated water volumes and carbon stocks of Alpine pro-glacial areas from the land cover map produced in this study.

Water volumes were obtained from empirical surface–volume scaling relations of the form: (1) V = exp(a_1) x A^b_1 (see ref. [29]) for lakes smaller than 28 ha, and (2) V = a_2 × A^b_2 (see ref. [103]) for lakes larger than 28 ha ; where V is the lake volume (x1e6 m³), A is the lake area (m²), and $a_{1/2}$ and $b_{1/2}$ are empirically derived constants (Fig S12). We chose to use two different scaling relations over this specific area range to respect the validity range of the empirically derived relations. Lake entities from our land cover have been defined as each ensemble of water classified pixels with an 8-connectivity pattern. Volume uncertainties have been derived accounting for water area mapping error assessment, as well as scaling relations uncertainties that we estimated from the relations' residuals in different area ranges. For the few lakes smaller than the lower bound of the scaling relation (1), we applied a ±100% uncertainty on the estimated volume. This overall method allowed us to derive a first-order estimate of current water retention in postglacial lakes in the Europeans Alps.

To estimate the carbon storage of postglacial ecosystems across the Europeans Alps, we used a simple cross product between the land cover map derived ecosystems area and first order empirical carbon density values accounting for above- and below-ground biomass, litter layer, and soil organic carbon. Following literature-supported values of alpine ecosystems [104,105,106,107,108], we assigned the following carbon density value (and uncertainty) to each of our land cover classes definition: bare lands: 5±5 tC/ha ; grassland: 60±10 tC/ha ; sparse vegetation: 30±5 tC/ha (assumed to be 50% of grassland value to account for low biomass and limited soil development); shrubland: 80±20 tC/ha ; and forest: 120±20 tC/ha. Estimates of carbon storage account for land cover area uncertainties (see Table S4).

Human infrastructures and protected areas

To assess the protection status of the end-of-LIA glacier extents in the European Alps, we intersected its coverage with the World Database on Protected Areas (WDPA)[42] that lists protected areas worldwide. We defined five groups of protected areas according to their theoretical protection enforcements, following the International Union for Conservation of Nature (IUCN) categories: (1) protected areas classified IUCN categories Ia (strict nature reserves), Ib (wilderness areas) and II (national parks), the strongest protection status ; (2) IUCN categories III (Natural monuments or features) and IV (Habitats or species management areas) ; (3) UNESCO World Heritage sites ; (4) all other protected areas that do not fit within the previous

groups (i.e., including IUCN categories V and VI) ; and (5) areas with no protected status at all. The WDPA database is updated monthly with submissions from governments, non-governmental organizations, landowners, and communities. Commonly accepted to be the most complete and up to date database; its completeness is subject to these external contributions, and some national to regional specificities might still be absent. We used data from October 2025 to which we added the Swiss "Federal Inventory of Landscapes and Natural Monuments" (ILNM), the only Federal Inventory missing as compared to the official country database [https://map.geo.admin.ch/], categorized as IUCN V, and covering a large proportion of the end-of-LIA glacier extents. The resulting surface and percentage of protected areas covering the end-of-LIA glacier extents is obtained after merging all protected areas within a given group (see Table S5, S6 and S7), i.e., spatial overlaps between groups being still possible, and real. This analysis provides a spatial assessment of formal protection coverage and protection categories, rather than an evaluation of legal effectiveness or management outcomes. IUCN categories were used as indicators of nominal protection status and management objectives, but they do not measure enforcement capacity, governance quality, ecological effectiveness, or the degree to which postglacial ecosystems are explicitly considered in management plans. We therefore interpret these results as a map of protection coverage and formal protection level across end-of-LIA glacier extents, not as a quantitative assessment of the effectiveness of individual protected-area instruments.

To assess the extent and distribution of anthropogenic pressures on 2015 glacial and postglacial areas in the European Alps, we mapped major human infrastructures intersecting with the end-of-LIA glacier extents. We focused on two primary land use types with significant environmental impact in high-altitude contexts: ski resort infrastructures and hydropower facilities. Our selection criteria are the following: we selected only infrastructures with a footprint inside the end-of-LIA glacier extents and accounted only for the portion inside the 2015 glacial and postglacial areas. We used OpenSkiMap.org[109] an open access database for ski areas, runs and lifts around the world, to map groomed ski runs and lifts having a footprint within the end-of-LIA glacier extents. The resulting dataset gives the length of each ski resort infrastructure detailed by country, and by deglaciated and glacierized areas (see Table S8). We used the Global Dam Watch (GDW v1) hydropower facilities dataset[110], completed by visual inspection of Google Earth and ESRI World imagery that added 8 missing facilities: 5 in Switzerland, 2 in Austria, and 1 in Italy- to list the number of hydropower facilities impacting postglacial areas (see Table S10). We limited the associated artificial water surfaces to the areas contained within the end-of-LIA glacier extents. Most hydropower lakes are thus larger than accounted for here. Because OpenStreetMap and Global Dam Watch are open datasets with variable completeness among countries and regions, we interpret infrastructure intersections as conservative estimates of mapped infrastructure presence rather than exhaustive inventories. The analysis is spatial rather than chronological: it identifies ski and hydropower infrastructure located within terrain exposed between the end of the Little Ice Age and 2015, but does not determine whether each feature was built before or after 2015, because construction dates were not consistently available across infrastructure types and countries.

Data availability

Landcover maps of the end-of-LIA deglaciated areas and adjacent zones, end-of-LIA glacier extents, and processed data are available via Zenodo at: https://zenodo.org/records/18623087. The ski resorts data is available at: https://openskimap.org/. The Global Dam Watch dataset is available here: https://www.globaldamwatch.org/. The World Database on Protected Areas (WPDA) is available here: https://www.protectedplanet.net/en.

Code availability

The codes and computational notebooks used to process Sentinel-2 data and perform landcover classification are available via Zenodo at: https://zenodo.org/uploads/18623290

Methods references

59. Nicolussi, K., Roy, M. Le, Schlüchter, C., Stoffel, M. & Wacker, L. The glacier advance at the onset of the Little Ice Age in the Alps: New evidence from Mont Miné and Morteratsch glaciers. *Holocene* **32**, 624–638 (2022).

60. Mourey, J. *et al.* A glacier inventory for the last Little Ice Age maximum in metropolitan France. *submitted to scientific data*.

61. Menounos, B. *et al.* Glaciers in Western Canada-Conterminous US and Switzerland Experience Unprecedented Mass Loss Over the Last Four Years (2021–2024). *Geophys. Res. Lett.* **52**, e2025GL115235 (2025).

62. Huss, M., Bauder, A., Barandun, M., Hodel, E. & Linsbauer, A. GLAMOS, 2026. Swiss Glacier Bulletin 2025. *Annual report No. 146* 0–26 (2026) doi:10.18752/glbulletin_2025.

63. Bai, Y. & Cotrufo, M. F. Grassland soil carbon sequestration: Current understanding, challenges, and solutions. *Science (1979).* **377**, (2022).

64. Siegfried, L., Vittoz, P. & Lane, S. N. Hydrological heterogeneity and the plant colonization of recently deglaciated terrain. *Arct. Antarct. Alp. Res.* **55**, (2023).

65. Carrivick, J. L., Heckmann, T., Turner, A. & Fischer, M. An assessment of landform composition and functioning with the first proglacial systems dataset of the central European Alps. *Geomorphology* **321**, 117–128 (2018).

66. Karra, K. *et al.* GLOBAL LAND USE/LAND COVER WITH SENTINEL 2 AND DEEP LEARNING. *International Geoscience and Remote Sensing Symposium (IGARSS)* **2021-July**, 4704–4707 (2021).

67. Zhang, X. *et al.* GLC_FCS30: Global land-cover product with fine classification system at 30ĝ€¯m using time-series Landsat imagery. *Earth Syst. Sci. Data* **13**, 2753–2776 (2021).

68. Friedl, M. A. *et al.* Medium Spatial Resolution Mapping of Global Land Cover and Land Cover Change Across Multiple Decades From Landsat. *Frontiers in Remote Sensing* **3**, (2022).

69. Zanaga, D. *et al.* ESA WorldCover 10 m 2021 v200. https://doi.org/10.5281/ZENODO.7254221 (2022) doi:10.5281/ZENODO.7254221.

70. Inglada, J. *et al.* Operational High Resolution Land Cover Map Production at the Country Scale Using Satellite Image Time Series. *Remote Sens. (Basel).* **9**, 95 (2017).

71. Malinowski, R. *et al.* Automated Production of a Land Cover/Use Map of Europe Based on Sentinel-2 Imagery. *Remote Sensing 2020, Vol. 12,* **12**, 1–27 (2020).

72. Venter, Z. S. & Sydenham, M. A. K. Continental-scale land cover mapping at 10 m resolution over europe (Elc10). *Remote Sens. (Basel).* **13**, (2021).

73. Marsoner, T., Simion, H., Giombini, V., Egarter Vigl, L. & Candiago, S. A detailed land use/land cover map for the European Alps macro region. *Sci. Data* **10**, (2023).

74. Huang, X. *et al.* A 10 m resolution land cover map of the Tibetan Plateau with detailed vegetation types. *Earth Syst. Sci. Data* **16**, 3307–3332 (2024).

75. Bayle, A., Carlson, B. Z., Thierion, V., Isenmann, M. & Choler, P. Improved mapping of mountain shrublands using the sentinel-2 red-edge band. *Remote Sens. (Basel).* **11**, (2019).

76. Bayle, A. *et al.* Uncovering the distribution and limiting factors of Ericaceae-dominated shrublands in the French Alps. *Front. Biogeogr.* **16**, (2024).

77. Gitelson, A. A., Keydan, G. P. & Merzlyak, M. N. Three-band model for noninvasive estimation of chlorophyll, carotenoids, and anthocyanin contents in higher plant leaves. *Geophys. Res. Lett.* **33**, (2006).

78. McFeeters, S. K. The use of the Normalized Difference Water Index (NDWI) in the delineation of open water features. *Int. J. Remote Sens.* **17**, 1425–1432 (1996).

79. Gorelick, N. *et al.* Google Earth Engine: Planetary-scale geospatial analysis for everyone. *Remote Sens. Environ.* **202**, 18–27 (2017).

80. Main-Knorn, M. *et al.* Sen2Cor for Sentinel-2. *https://doi.org/10.1117/12.2278218* **10427**, 37–48 (2017).

81. Montero, D. eemont: A Python package that extends Google Earth Engine. *J. Open Source Softw.* **6**, 3168 (2021).

82. Alemohammad, H. & Booth, K. LandCoverNet: A global benchmark land cover classification training dataset. http://arxiv.org/abs/2012.03111 (2020).

83. d'Andrimont, R. *et al.* Harmonised LUCAS in-situ land cover and use database for field surveys from 2006 to 2018 in the European Union. *Sci. Data* **7**, (2020).

84. Stanimirova, R. *et al.* A global land cover training dataset from 1984 to 2020. *Sci. Data* **10**, (2023).

85. Giuliani, G., Rodila, D., Külling, N., Maggini, R. & Lehmann, A. Downscaling Switzerland Land Use/Land Cover Data Using Nearest Neighbors and an Expert System. *Land (Basel).* **11**, (2022).

86. Scornet, E. Tuning parameters in random forests. *ESAIM Proc. Surv.* **60**, 144–162 (2017).

87. Stock, A. Choosing blocks for spatial cross-validation: lessons from a marine remote sensing case study. *Frontiers in Remote Sensing* **6**, (2025).

88. Sirén, J., Somervuo, P. & Ovaskainen, O. Agent-based versus correlative models of species distributions: Evaluation of predictive performance with real and simulated data. *Methods Ecol. Evol.* https://doi.org/10.1111/2041-210X.70016 (2025) doi:10.1111/2041-210X.70016.

89. Dormann, C. F. *et al.* Model averaging in ecology: a review of Bayesian, information-theoretic, and tactical approaches for predictive inference. *Ecological Monographs* vol. 88 485–504 Preprint at https://doi.org/10.1002/ecm.1309 (2018).

90. Vovk, V., Gammerman, A. & Shafer, G. Algorithmic learning in a random world. https://link.springer.com/content/pdf/10.1007/0-387-25061-1_8.pdf (2005).

91. Angelopoulos, A. N. & Bates, S. A Gentle Introduction to Conformal Prediction and Distribution-Free Uncertainty Quantification. http://arxiv.org/abs/2107.07511 (2021).

92. Valle, D., Izbicki, R. & Leite, R. V. Quantifying uncertainty in land-use land-cover classification using conformal statistics. *Remote Sens. Environ.* **295**, (2023).

93. Tottrup, C. *et al.* Surface Water Dynamics from Space: A Round Robin Intercomparison of Using Optical and SAR High-Resolution Satellite Observations for Regional Surface Water Detection. *Remote Sens. (Basel).* **14**, (2022).

94. Bhardwaj, A. *et al.* A lake detection algorithm (LDA) using Landsat 8 data: A comparative approach in glacial environment. *International Journal of Applied Earth Observation and Geoinformation* **38**, 150–163 (2015).

95. Pekel, J. F., Cottam, A., Gorelick, N. & Belward, A. S. High-resolution mapping of global surface water and its long-term changes. *Nature* **540**, 418–422 (2016).

96. Cordeiro, M. C. R., Martinez, J.-M. & Peña-Luque, S. *Automatic Water Detection from Multidimensional Hierarchical Clustering for Sentinel-2 Images and a Comparison with Level 2A Processors 3 4 Automatic Water Detection from Multidimensional Hierarchical Clustering for Sentinel-2 Images and a Comparison with Level 2A Processors*. (2020) doi:https://www.sciencedirect.com/science/article/abs/pii/S0034425720305824?via%3Dihub.

97. Peña-Luque, S. *et al.* Sentinel-1&2 multitemporal water surface detection accuracies, evaluated at regional and reservoirs level. *Remote Sens. (Basel).* **13**, (2021).

98. Serrano, C., Gardent, M., Bonnefoy-Demongeot, M., Thibert, E. & Richard, D. *Plan d'Actions Pour La Prévention Des Risques d'Origine Glaciaire Ou Périglaciaire*. www.irstea.fr (2019).

99. Mölg, N. *et al.* Inventory and evolution of glacial lakes since the Little Ice Age: Lessons from the case of Switzerland. *Earth Surf. Process. Landf.* **46**, 2551–2564 (2021).

100. Buckel, J., Otto, J. C., Prasicek, G. & Keuschnig, M. Glacial lakes in Austria - Distribution and formation since the Little Ice Age. *Glob. Planet. Change* **164**, 39–51 (2018).

101. Karger, D. N. *et al.* CHELSA-W5E5: Daily 1gkm meteorological forcing data for climate impact studies. *Earth Syst. Sci. Data* **15**, 2445–2464 (2023).

102. Copernicus DEM. *Copernicus DEM* Preprint at https://doi.org/10.5270/ESA-c5d3d65 (2022).

103. Cook, S. J. & Quincey, D. J. Estimating the volume of Alpine glacial lakes. *Earth Surface Dynamics* **3**, 559–575 (2015).

104. Ward, A., Dargusch, P., Thomas, S., Liu, Y. & Fulton, E. A. A global estimate of carbon stored in the world's mountain grasslands and shrublands, and the implications for climate policy. *Global Environmental Change* **28**, 14–24 (2014).

105. Canedoli, C. *et al.* Evaluation of ecosystem services in a protected mountain area: Soil organic carbon stock and biodiversity in alpine forests and grasslands. *Ecosyst. Serv.* **44**, (2020).

106. Canedoli, C. *et al.* Environmental factors influencing organic carbon stocks across different pools in alpine ecosystems. *J. Mt. Sci.* **21**, 4208–4222 (2024).

107. Agaba, S., Ferré, C., Musetti, M. & Comolli, R. Mapping Soil Organic Carbon Stock and Uncertainties in an Alpine Valley (Northern Italy) Using Machine Learning Models. *Land (Basel).* **13**, 78 (2024).

108. Rota, N. *et al.* Assessing the carbon stock in the Alps: Considerations on three different approaches. *J. Nat. Conserv.* **82**, (2024).

109. OpenSkiMap.org. https://openskimap.org/.

110. Lehner, B. *et al.* The Global Dam Watch database of river barrier and reservoir information for large-scale applications. *Sci. Data* **11**, (2024).

Acknowledgements

We warmly thank all the financial supports of the Ice&Life project (Foundation University Savoie Mont-Blanc, French Ministry of Ecology and the Erable Programme of the GIP EPAU, the foundations Le Poids du Vivant, Anyama, Lemarchand, Alpes Sauvage, Alter Colibris, Eau Neige Glace, 1% for the Planet France, Fondation de France, Kilian Jornet Foundation, Millet, Patagonia, Picture). We also thank Marion Sevaz, Laura Cantounet and Christophe Corona for their useful comments on the manuscript, as well as Manuel Brügger and Anna Stückelberger for helpful exchanges.

Author contribution

The original idea emerged from J.-B.B., F.A., S.C.-F., and J.C.C following discussions with M.H, M.F., and J.P. A.G. and A.B. designed the study. A.G. performed all the analysis with significant help from A.B. on the training dataset building and satellite indices computation, M.F. on glacier-related data, J.P. on carbon stock estimations. A.G. prepared the figures and tables. A.B. wrote the manuscript with significant

help from A.G. and with help of J.-B.B. and M.F. P.B. gave strong support on the legal aspects. All authors made substantial contributions to the final version of the paper.

Competing interests

The authors declare no competing interests.

Supplementary Files

This is a list of supplementary files associated with this preprint. Click to download.

- review1revisedsupplementaryfiles.docx